POST-FIRE HAZARD DETECTION USING ALOS-2 RADAR AND LANDSAT-8 OPTICAL IMAGERY

S. Mutai [1, *], L. Chang [2]

[1] International Fund for Agricultural Development, Kenya, stellachela1@gmail.com
[2]Dept. of Earth Observation and Science, ITC, University of Twente, The Netherlands, ling.chang@utwente.nl

Commission IV

KEY WORDS: Post-fire, SAR, SVM, Bushfire

ABSTRACT:

This study investigates the use of Advanced Land Observing Satellite 2 (ALOS-2) equipped with an enhanced L-band SAR sensor imagery alongside with Landsat-8 optical sensor in detection and mapping of burnt and unburnt scars occurring after a bushfire in Victoria, Australia. The bushfires had recently occurred in the period of 2018-2019. The analysis was explored using a contextual classifier Support Vector Machine (SVM), as SVM allows us to integrate spectral information and spatial context through the optimal smoothing parameter without degrading image quality. The training and test set datasets consisting of burnt and unburnt pixels were created from Landsat-8 scenes used as reference data. The backscatter intensity maps (acquired before and after the forest fires) from ALOS-2 data were compared and investigated, with a special concern on topographic influence removal. The dual polarizations (HH and HV) have been used to improve the forest fire mapping capability. These change detection techniques were based on image feature differences, index calculation such as normalized burn ratio. The burnt area and unburnt area were then classified via a threshold given by the pre- and post- disaster differences. The classification result achieved an accuracy of 80% Landsat-8 and 89% ALOS-2. This result shows the limitations of burnt area mapping with ALOS-2 due to effect local incidence angle and topography were of greater impact resulting in shadows. Nevertheless, the results in both areas verify the use of satellite SAR sensors and optical in forestry application.

1. INTRODUCTION

Forest is a key component of ecology and sustainable development and at the same time a dynamic resource. It is mainly affected by coexisting ecological processes, direct management interventions, and forest fires. Forest fires are generally referred to as wildfires due to their frequency and intensity (Westerling et al., 2006). The increased intensity during burning in tropical regions, temperate, and mountainous forests and the increasing trend in the occurrence of fire events in Victoria, Australia, as a result of climate change and weather, cause a variation in forest structure, species and global biomass burning, topography (Clarke et al., 2013). All this underlines the need for the development of a reliable procedure to accurately and rapidly map burnt areas. Satellite remote sensing has been used for detection, mapping, managing fire-prone areas and estimating the severity and intensity of bushfires (Yebra et al., 2013). In particular, optical satellite data have been extensively used and proved to be useful for mapping of burnt areas (Koutsias et al., 2000; Roy et al., 2002; Gitas et al., 2012). However, the optical data has a disadvantage of being hindered by cloud cover or smoke during fire instance and errors due to spectral overlap (Cocke et al., 2005; Allison et al., 2016). Cloud cover reduces the observation rate in the visible/infrared bands which when depicting low fire severity and fast vegetation regrowth after fire may cause low spectral separability between burnt and unburnt zones (Mouillot et al., 2014).

In contrast, Satellite Synthetic Aperture Radar (SAR) imagery has the ability to penetrate clouds and fire smoke providing invaluable information on burnt areas (Hoekman et al., 2010). Its weather independency also is an advantage compared to optical sensors. SAR has widely been used for biomass estimation, vegetation mapping and also ecological monitoring and growth (Kumar et al., 2017). SAR has not only been used for various ecological applications, such as vegetation mapping and biomass estimation (Kasischke, 1997; Kasischke et al., 2000), but has also been used for burnt area mapping, given that the backscatter signal is sensitive to vegetation structure and biomass: removal of leaves and branches from trees due to fire alters the scattering mechanisms causing temporal variations of the backscatter coefficient (Bourgeau et al., 2002). The effects of fires on the backscatter coefficient have been exploited in several fire-related studies. This includes identification of fires scars in boreal forestry by exploiting the C-band backscatter of burnt areas (Bourgeau et al., 2010). The research on boreal forest depicted stronger return of backscatter intensity from burnt scares as compared with the unburnt, which is in response to changes in moisture content (Tanase et al., 2014). Similar observations were made in tropical rain forest environment but discovered under dry weather decrease in backscatter compared to wet conditions however the discrimination of burnt and unburnt areas was difficult (Huang & Siegert, 2004). Some studies also reported the use of SAR in the mapping of burnt scars in the Mediterranean and the influence on rainfall in backscatter coefficient (Menges et al., 2004). However, most of the reported studies have focused on the detection and mapping of fire severity using SAR and very

* Corresponding author

few have highlighted a major issue in utilizing SAR backscatter such as the effect of biophysical parameters with great impact from local topography (Sivasankar et al., 2015). Few studies have been done on the effect of geographical aspect of an area, its influence on local topography which directly affects backscatter intensity in the retrieval of burnt and unburnt areas after a bushfire.

This research aims to analyze the use of backscatter intensity in the retrieval of burnt and unburnt areas in relation to the geographical aspect of the study area. In this endeavor, we attempt to analyze the effect of bushfire on hilly-mountainous areas in Australia, and compare the use of satellite SAR and optical imagery in the identification of burnt and unburnt patches within fire perimeter zones.

2. METHODS

2.1 Processing flowchart

To detect and classify the burnt areas after fires, we carry out the processing flowchart in Figure 1, which includes initial pre-processing (Small. 2011), and contextual classification using support vector machine method, assisted by optical (reference) data. The deliverable – land cover map includes burnt and unburnt classification map and fire severity map. The following subsections present the relevant methods that we apply.

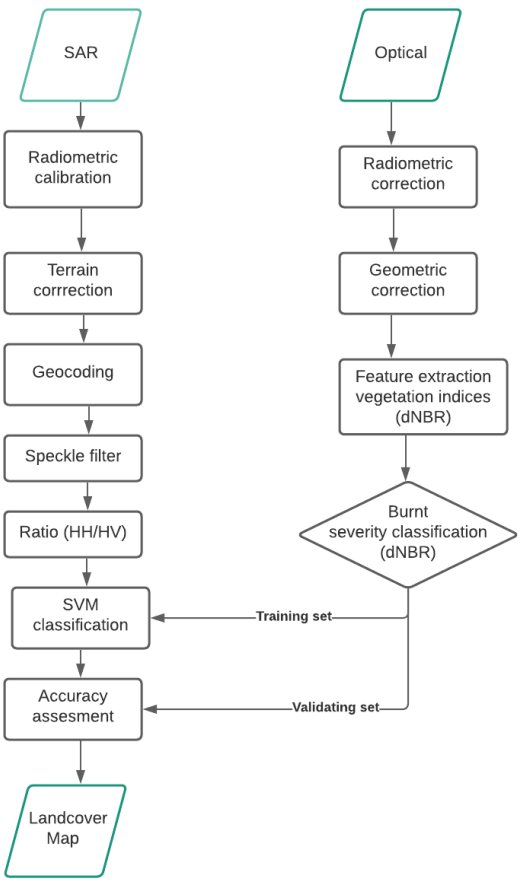

Figure 1. Processing flowchart

2.2 Burnt sensitive spectral composite

To define a reference for the precise detection of burnt and unburnt areas using optical imagery, we use the spectral index normalized burnt ratio (*NBR*) (Escuin et al., 2008). The *NBR* formula relates similarly to the normalized difference vegetation index (*NDVI*), and is formed as

$$NBR = (NIR - SWIR) \cdot (NIR+SWIR)^{-1}, \quad (1)$$

where the *NIR* (near-infrared) covers 750-900 nm and shortwave infrared (*SWIR*) which covers 2080-2350 nm portion of the electromagnetic spectrum (Allison et al., 2005). The *NIR* reflects strongly in vegetation while the *SWIR* is lower, but after the fire, the *SWIR* reflects stronger than the *NIR*. The contrasted relation between *SWIR* and *NIR* over burn scar and healthy vegetation is used to identify burnt vegetation by the help of *NBR*.

The *NBR* difference (d*NBR*) in pre- and post- fire can be used to measure forest regeneration with time aspect, shown as

$$dNBR = preNBR - postNBR. \quad (2)$$

In general, the burnt severity levels can be categorized as five major classes: unburnt areas, lightly burnt areas, medium burnt areas and, deeply burnt areas and, post-fire regrowth (Allison et al., 2005). The burnt severity levels are used as input to machine learning (ML) algorithms, support vector machine for our case.

2.3 Support vector machine (SVM)

In recent decades, Support Vector Machine (SVM) came out as a very popular supervised machine learning algorithm of classification and regression and its concept introduced by (Cortes & Vapnik, 1995). It is a statistical learning algorithm that finds an optimal hyperplane and maximizes the margin between two defined classes using fewer training samples (Vapnik, 2006). SVM tends to maximize the margin between the hyperplane and the training samples while minimizing the empirical error caused by the training samples. The learning is an iterative process of finding a decision boundary that separates the training patterns (Zhu & Blumberg, 2002). The maximum margin has selected as a decision boundary. On the basis of this distance or margin, the objects are separately having different class memberships. A subset of data named as support vector determines the position of boundary (Richards & Jia, 2006). In the present study, the most used Radial Basis Function (RBF) kernel of SVM was employed to classify the burn and unburn patches. RBF is selected as the optimal kernel in its parameter adjustments according to classifier performances and a one-against-one (OAO) strategy is used to handle multi-class problems (Kavzoglu & Colkesen, 2009).

2.4 Training data processing

A training dataset preparation method is the backbone of supervised machine learning techniques to solve classification and regression problems (Chi et al., 2008). Training set contains two-thirds of the total area and test set one third. The main objective of the study is to identify burn and unburn patches, therefore to train the algorithms in two categories (burn and unburn) of sample dataset is required. The band combination of *SWIR*, *NIR* and Blue could highlight the burn pixels from healthy and unburn vegetation. The RGB color composites of images before and after fire can be used as sampling site to identify the classes. Additionally the Victoria database shape

file (more detail in section 3) can be utilized to generate effective and accurate training sample data.

2.5 Accuracy assessment and validation

Validation is an essential part of any classification as it assesses the accuracy of results and we can tell the correctly and not correctly classified pixels in the image. The validation sets are chosen with reference to the vegetation index (d*NBR*) which is used in the detection of burnt and unburnt areas by computing the difference of two images (pre/post) fire images as shown in Eq. (2). They are segmented to extract burnt and unburnt areas. According to Madoffe et al. (2000), it defines unburnt areas as having the forest fire not burning forest floor, lightly burnt areas are partially burnt and scorched trees and burn is Scottish. They further described that moderately burnt area are whereby most vegetation is burnt to ground level and most forest floor coverage is burnt while deeply or highly burnt areas and the forest floor is consumed by combustion and skeletons of vegetation's are left as remnants. A random feature selection of test sets is suggested to be used to reduce data redundancy. Validation dataset is used to test the ability of the SVM classifier to classify new pixels in new datasets. Finally, the results obtained are validated using training and test sets to produce overall accuracy. The classification results are evaluated by accuracy assessment accuracy takes into consideration the overall accuracy (OA), users' accuracy (UA), producers' accuracy (PA) and kappa coefficient (Kc) which uses the error matrix incorrectly classified pixels. Present study has performed some set of accuracy assessment techniques i.e. User Accuracy (UA) which corresponds to error of commission or exclusion (from user perspective), Producer Accuracy (PA) address the omission or inclusion errors (point of view of the map maker). The Kappa (K) reflects the dissimilarities between actual agreement and expected. Whereas the Overall Accuracy (OA) is the simplest statistics, which is calculated by dividing the correct pixels by total pixels (Foody, 2010).

3. STUDY AREA AND DATA DESCRIPTION

3.1 Study area

The study area (Area of Interest (AOI), in blue) selected for our research was Victoria, Australia, see Figure 2 in blue. The choice of our study areas was influenced by the following factors, firstly it experiences severe wildfires occasionally that have caused massive impact on human lives and economic and environmental degradation. Thus, it would be key to look into the causes of fire and the measures to be undertaken to mitigate future fires and also for sustainability of the forest ecology. Secondly, it has a forest structure that influences the spread of fire rapidly. Thirdly it has varying geographical phenomena that would be of interest in our research in understanding how the area responds to fire occurrences. Fourthly it has recent forest fire occurrences that could be of interest in our research. Lastly the availability of ALOS-2 data and Landsat-8 dataset would be suitable and available for study area.

3.2 Victoria bushfire data

The Victoria bushfire database was used, which contained bushfires registered and updated from 1939 to 2018 (Victoria, 2018). The database contained information in vector shape file format of all the burns and bushfires in the area, occurrence time, the level of severity, location of the fire, fire type, season, area coverage and method of obtaining the fire perimeters together with accuracy in the resolution of the method used. From the dataset one bushfire was extracted between 2018 and 2019 using a criterion that it was a bushfire, its occurrence date was recent (2018/2019) and their burnt severity level was the highest in the database. Example is shown in red in Figure 2.

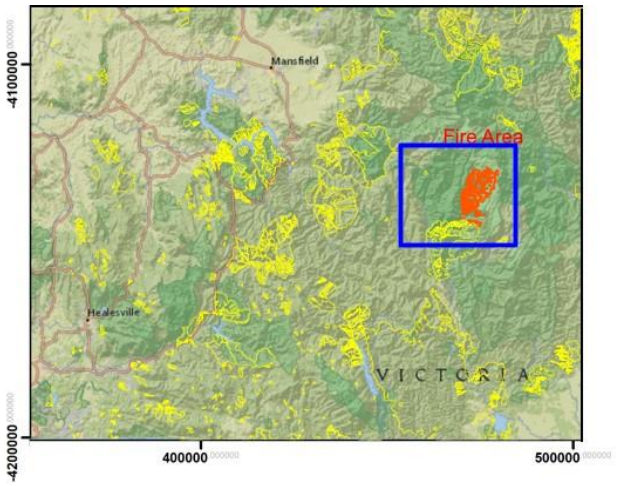

Figure 2. Bushfires and controlled burns between 2015 and 2020 (in yellow), from the Victoria bushfire database. In red: fires selected for this study in period 2019/2020. Map source: National Geographic, Esri, Garmin, HERE, UNEP-WCMC, USGS, NASA, ESA, METI, NRCAN, GEBCO, NOAA, increment P Corp. The study area is indicated in blue.

3.3 ALOS-2 data

A pair of ALOS-2 data (L1.5) obtained in ascending orbit, acquired on 30 July 2019 (before fire), 08 October 2019 (after fire) were used. The signal wavelength of ALOS-2 is 24 cm, in L-band. Each ALOS-2 image has a dual polarimetric channel, with HH and HV. The spatial resolution of ALOS-2 is 10 x 10 m. Figure 3 illustrates the pre-fire and post-fire intensity maps over the AOI in HH mode.

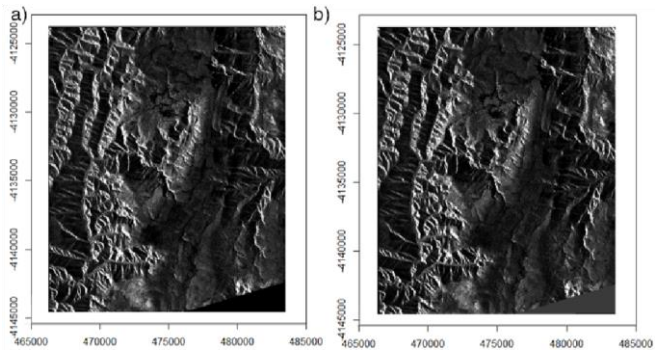

Figure 3. ALOS-2 pre-fire (a) ([-0.47, 63.01] dB in HH) and post-fire (b) ([-0.44, 47.13] dB in HH) intensity images covering the area of bushfires, respectively.

3.4 Landsat-8 data

Two Landsat-8 Operational Land Imager (OLI) for the period 2019 images, separately acquired on 26 July 2019 (before fire) and 13 October 2019 (after fire), were used. Both images have <15% cloud coverage, and with 30 m spatial resolution. We deliberately collected data in the mid-dry (October to

December) season in Australia during which skies are clearer and most satellite images are of good quality. Figure 4 shows pre-fire and post-fire false color composite maps over the AOI.

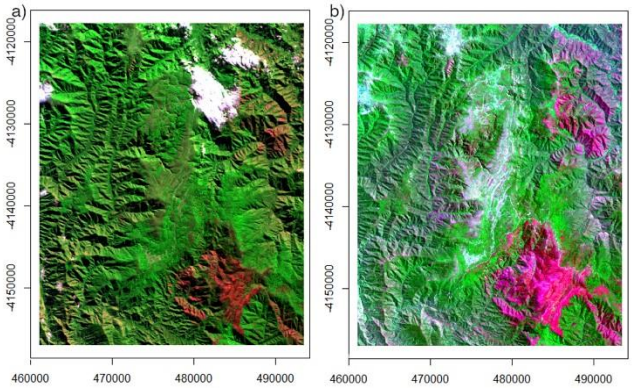

Figure 4. Landsat-8 pre-fire (a) and post-fire (b) images covering the area of bushfires, respectively. Band combination is R:G:B=7:5:2. Foreshowing changes before and after fire.

4. RESULTS AND DISCUSSION

4.1 Optical-based spectral indices (d*NBR*) calculation

Fire scar differentiation using optically based indices was attainable in analyzing the bushfire data. The burnt severity estimation was accurate for highly burnt sites and medium burnt sites however for low and unburnt sites there was a classification error. The threshold-based classification of d*NBR* was used as a methodological reference to obtain burnt severity maps. The burnt severity using Landsat-8 data was developed by comparing pre and post-fire satellite images as this showed the capability of different spectral bands in burnt area detection. The burnt ratio index was found to be sensitive to regenerate vegetation and also showed forest regeneration is slower especially in areas where the degree of burnt severity was high. The results obtained from d*NBR* show that the unburnt pixels depict very low optimal values that are close to zero. In regard to burnt pixels, the optimal values of *dNBR* are considerably high reaching a mean value of 1.32. The categories used in the index were classified into five classes as shown in Table 1. A bigger proportion of the bushfire lied between medium to highly burnt areas. However,it was noted that the burnt severity levels consisted of classification error especially between the high and medium burnt areas were difficult to separate two classes and also between the unburnt and low burnt areas.

d*NBR* Values (not scaled)	Burn Severity
-0.500 to -0.251	Enhanced Regrowth, high (post-fire)
-0.250 to -0.101	Enhanced Regrowth, low (post-fire)
-0.100 to +0.99	Unburnt
+0.100 to +0.269	Low severity burn
+0.270 to +0.439	Moderate to low severity burn
+0.440 to +0.659	Moderate to high severity burn
+0.660 to +1.300	High severity burn

Table 1. Burn severity levels obtained calculating d*NBR*, proposed by United States Geological Survey (USGS).

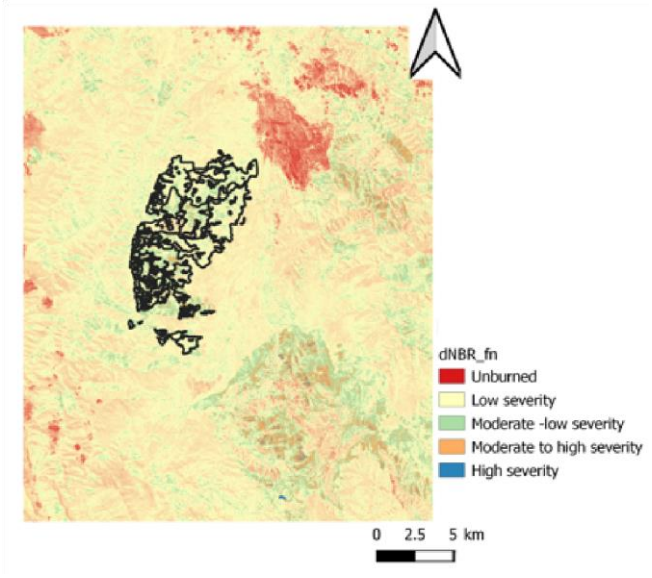

Figure 5. Difference normalized burnt ratio (d*NBR*) from Landsat-8 of the AOI.

4.2 Synergistic use of optical and radar data

A backscatter and reflectance analysis of burnt and unburnt patches was applied to the ALOS-2 and showed highly different values over burnt areas compared to the unburnt areas. The data showed only slightly higher backscatter values over burnt areas compared to the unburnt areas, the backscatter analysis showed a clear increase over the burnt areas compared to the pre-disaster image which turned out as sufficient for burnt area detection. The ALOS-2 co-polarized backscatter (HH) increased with burnt severity while the cross-polarized (HV) backscatter decreased with burn severity. Low sensitivity to forest regrowth was observed for the L-band backscatter with most of it classified as burnt areas. This is because of burnt leaves, branches and tree trunks at some areas leaving bare soil area. A major issue in the use of ALOS-2 image was the influence of topography and local incidence angle on the backscatter coefficient during mapping of burnt and unburnt areas. It was difficult to separate the burnt severity levels using the ALOS-2 due to the transitional nature of the fire. All the burn severity levels largely overlap each other. However, we reclassified the burnt severity level to two classes burnt and unburnt class as shown in Figure 6 which shows a stronger return of burnt and unburnt patches compared to optical dataset shown in Figure 7, due to the high influence of geometry acquisition and hilly terrain. Landsat-8
utilizes the spectral sensitivity of defined classes which take the measure of only the vegetation fill and crown closure while ALOS-2 utilizes the polarimetric sensitivity of removal of crown leaves, branches.

However, the optical Landsat-8 showed a stronger sensitivity to changes resulting after the fire compared to ALOS-2 data. This is proved by the visual assessment of the RGB image of optical data as shown in Figure 4. Nevertheless, Landsat-8 classification resulted in a similar match with the fire extent of the polygon showing the spectral sensitivity of pixels to changes after the fire similarly to ALOS-2 foreshowing the capability of both radar and optical in mapping burnt areas. Note that for classification with the SVM method, we collected 33 and 30

training data samples, and 22 and 20 test samples for ALOS-2 and Landsat-2 images, respectively.

To assess the certainty of our results in the separation of burnt and unburnt areas in both optical and radar we used kappa coefficient. Both the producer accuracy and user accuracy were taken into consideration as shown in Table 2. The remote sensing indices that accessed burnt versus unburnt areas produced better overall accuracy, higher user and producer accuracy results as shown in Table 2 through SVM classification of radar and optical. This showed the capability of both the electromagnetic spectrum and SAR backscatter intensity in corresponding to changes in vegetation structure after a fire. Similarly, we obtained quite a good classification percentage accuracy and separation of burnt and unburnt areas within fire perimeter zones as shown.

Data	Kappa coefficient	Producer accuracy	User accuracy
ALOS-2	0.89	Burnt=80.69% Unburnt=78.65%	Burnt=85.65% Unburnt=80.25%
Lansat-8	0.80	Burnt=84.35 % Unburnt=82.26%	Burnt=92.43% Unburnt=84.65%

Table 2. Accuracy assessment results based on kappa statistics from SVM classification of SAR and optical over the AOI.

It was seen in particular after classification with SVM the vector shape file that represents fire perimeter zone was not exactly fitting the all burnt zones depicted in classification results. The problem could be related to the timing of digitization of vector fire perimeter which might have occurred at early stages of the while our spectral classification analysis was related to the post-fire analysis of the image. This may lead disparity of fire perimeter shape file with the actual ground timing of fire timeout as shown in Figure 5. This possibly reflected the start of the fire but did not execute the whole fire zone. Thus, it was a limiting factor in determining whether the area was burnt or unburn while obtaining training sets.

5. DISCUSSION AND CONCLUSION

In relation to the aim of our research as mentioned in the introduction is to characterize the difference in burnt and unburnt scars using remote sensing methods comparing ALOS-2 and Landsat-8. The extent of severity of the fire was explored firstly by use of vegetation indices dNBR from Landsat-8 imagery and resulted in the identification of burnt and unburnt patches in Victoria, Australia. The comparison of pre- and post-fire reflectance values showed spectral similarity as there was a decrease in the post-fire values indicating complete or partial loss of vegetation based on fire intensity, see Figure 6 and Figure 7. The differences at burnt severity maps displayed in Figure 5 particularly at intermediate severity levels point out the classification errors that eventually affect the overall accuracy result. The spectral confusion has been commonly reported by various authors (Sunderman & Weisberg, 2011; Quintano et al., 2018). These changes were highly influenced by the timely acquisition of the images as this is a key component in relation to the start of fire dates and sampling of the vegetation changes.

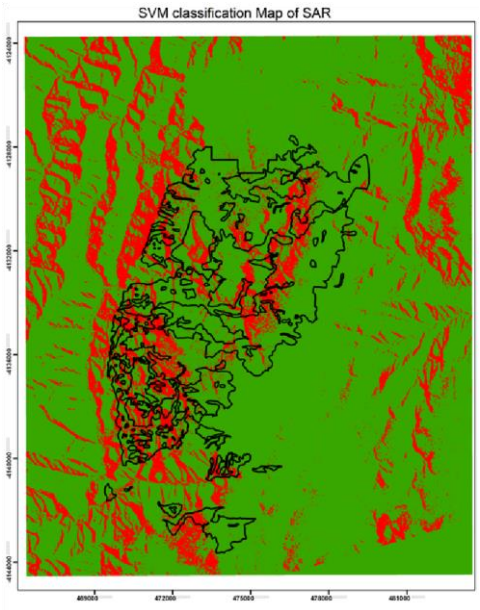

Figure 6. Classified map of ALOS-2 imagery of study area. Red colour representing burnt areas and green representing unburnt areas.

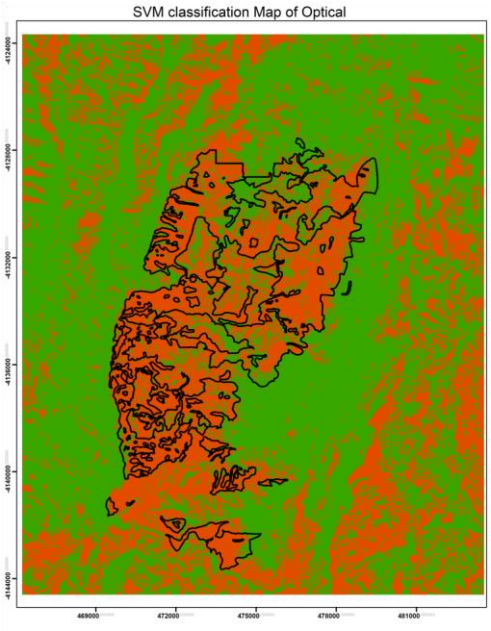

Figure 7. Classified map of Landsat-8 optical imagery of study area. Red colour representing burnt areas and green representing unburnt areas.

Secondly was to analyze the use of satellite SAR imagery in polarimetric aspect and backscatter intensity. This resulted in discrimination of burnt areas from the unburnt areas and provided distinct information that was related more to changes in the forest structure as shown in section 4.1. The changes were mainly associated with the backscatter intensity of the fire resulting from changes in vegetation structure and also topography similar results obtained from (Siegert & Ruecker, 2000). However, the influence of local incidence angle and topography was of considerable effect resulting in shadows. Thus the analysis of combination of the polarimetric aspect and backscatter intensity could not be validated in some hilly areas, and the resultant difficulty in discriminating whether the areas

were burnt or unburnt leads to commission and omission errors (Sun & Ranson, 2015).

Thirdly the determination of the degree of spectral contrast between the burnt and unburnt areas was performed. This was done by assessing the use of kappa coefficient. Both the producer accuracy and user accuracy were taken into consideration as shown in Table 2. The remote sensing indices that accessed burnt versus unburnt areas produced better overall accuracy, user and producer accuracy. This showed the capability of the electromagnetic spectrum to correspond to changes in vegetation after fire. Nevertheless, it was important to note that overall accuracy obtained could not be relied upon as it could be biased on the sample size of one class in relation to the other (Benson, 2005). This is clearly shown with the *dNBR* values whereby the bright areas within and outside fire perimeter zones were classified as burnt areas even though some of the were unburnt areas such as rocky areas and buildings outside fire perimeter zone. However, keen attention should be kept when relating to the accuracy assessment result and expected the outcome of defined classes. Also, validation maps or existing forms of information on the land use of the patches of holes that remain unburnt would help in understanding its influence on fire regeneration.

Finally, the differences in the sensitivity of fire for SAR and optical varied and this has been addressed in section 4.2. However, an in-depth in time series analysis would be efficient in understanding the structural and behavioral changes caused by fire, despite the intensity of the fire. In relation to the vegetation changes past and recent analysis of wildfire behavior relates it to the rate of fuel consumption, weather, and topography. A clear understanding should be brought forth on how fire ignition points influence the direction of fires based on wind pattern (Fischer et al., 2015).

Regarding the societal impact, our results would be helpful to various stakeholders based on their interests. The main stakeholders being state forest agencies including state government departments, community or landowners and finally, firefighters, risk emergency providers, and forest managers. We could see the state government departments who are keen on forest management use the spatial mapping of bushfire coverage and remote sensing analysis of fire severity act as a guide in providing emergency resources in most affected areas. Also, they would create restricted boundaries surrounding frequent bushfire zones that should not be inhabited as a measure of safety of human and ecological preparedness. Community and landowners that reside within and close to the fire forested zones could be educated on the factors that aggregate and influence the fast spread of bushfire, the particular zones that are highly susceptible to fire and should be avoided and the impact of fire to their physical health and economic wealth. Firefighters and risk emergency providers would benefit from the study by additional integration of fire ignition points in developing fire escape zones and setting up of fire emergency units. Forest managers would benefit in decision making on how to minimize adverse impacts caused by the bushfire in relation to unburnt areas that may act as reignition points of fire again. They would also use the information from radar to understand the influence of forest type and structure to fuel connectivity and use it to adequately allocate resources to manage fire risks in an effective and safe manner.

6. RECOMMENDATION

The results of this study confirmed there was a difference between the backscatter intensity and spectral aspect in the analysis of burnt and unburnt areas, especially in Australian bushfires. Scattering from the tree crown was the most predominant of the backscatter for the forested areas at L-band. However, the backscatter intensity was highly dependent on environmental conditions such as terrain effect and also on the local incidence angle. This affected the separation of burnt and unburnt areas.

As a future scope, we recommend to incorporate the effects of topography in the analysis. With an idea of the variations in mechanical influences, it is possible to track the spatial orientation of bushfires and the regions that are more susceptible to the spread. This will also provide vital information about the nature and susceptibility of forests to fire. Moreover, such topographic analysis when augmented with spatial statistics can be of great potential in predicting the future fire events in a reliable manner. We further suggest to include the uncertainty propagation from multi source remote sensing data in an attempt to link the error budget with the operational issues, which can be carried out by the forest officials to control and prevent such events.

Further recommendation in the research would be an enhanced data fusion of SAR and optical imagery from multiple satellites in order to improve the timeliness and accuracy of burnt area mapping. The information derived from different microwave bands (C-, L-, and/or P- bands) needs to be investigated since it could lead to a more detailed understanding of forest fires and to a further improvement of mapping accuracies. Explore other target decomposition theorems and compare its results to the Cloud and Pottier decomposition theorem and see its effectiveness in burnt severity estimation compared to vegetation indices. Lastly further method improvement of terrain correction upon SNAP software for ALOS-2 is required, so that one can perform polarimetric decomposition or use alternative tool(s) to improve the quality of the results.

ACKNOWLEDGEMENTS

The authors thank dr. Valentyn Tolpekin (ICEYE) for giving valuable advice and sharing R scripts, JAXA for providing ALOS-2 data under the project ‘Analysis of forest fire using Radar’ [ER2AN126], and the United States Geological Survey for providing Landsat-2 data.

REFERENCES

Allison E. Cocke, Peter Z. Fulé, J. E. C. (2005). Comparison of burn severity assessments using dNBR and ground data, 189–198.

Allison, R. S., Johnston, J. M., Craig, G., & Jennings, S. (2016). Airborne optical and thermal remote sensing for wildfire detection and monitoring. *Sensors (Switzerland)*, *16*(8). https://doi.org/10.3390/s16081310

Benson, K. &. (2005). Landscape assessment: ground measure of severity, the composite burn index, and remote sensing of severity, the normalized burn index. In: Lutes, D., Keane, R., Caratti, J., Key, C., Benson, N., Sutherland, S., Gangi, L. (Eds.). *FIREMON: Fire Effects Monitoring and Inventory System, Rocky Mountains Research Station, USDA Forest Service: Fort Collins, CO, USA, PP. 1–51.*, 1–55.

https://doi.org/10.1002/app.1994.070541203

Bourgeau-Chavez, L. L., Kasischke, E. S., Brunzell, S., Mudd, J. P., & Tukman, M. (2002). Mapping fire scars in global boreal forests using imaging radar data. *International Journal of Remote Sensing*, *23*(20), 4211–4234. https://doi.org/10.1080/01431160110109589

Bourgeau-Chavez, L. L., Kasischke, E S, Brunzell, S., Mudd, J. P., Tukman, M., (2010). Mapping fire scars in global boreal forests using imaging radar data, *1161*. https://doi.org/10.1080/01431160110109589

Chi, M., Feng, R., & Bruzzone, L. (2008). Classification of hyperspectral remote-sensing data with primal SVM for small-sized training dataset problem. *Advances in Space Research*, *41*(11), 1793–1799. https://doi.org/10.1016/j.asr.2008.02.012

Clarke, H., Lucas, C., & Smith, P. (2013). Changes in Australian fire weather between 1973 and 2010. *International Journal of Climatology*, *33*(4), 931–944. https://doi.org/10.1002/joc.3480

Cocke, A. E., Fulé, P. Z., & Crouse, J. E. (2005). Comparison of burn severity assessments using Differenced Normalized Burn Ratio and ground data. *International Journal of Wildland Fire*, *14*(2), 189–198. https://doi.org/10.1071/WF04010

Cortes, C., & Vapnik, V. (1995). Support-Vector Networks. *Assembly*, *44*(13), 97. https://doi.org/10.1111/j.1747-0285.2009.00840.x

Escuin, S., Navarro, R., & Fernández, P. (2008). Fire severity assessment by using NBR (Normalized Burn Ratio) and NDVI (Normalized Difference Vegetation Index) derived from LANDSAT TM/ETM images. *International Journal of Remote Sensing*, *29*(4), 1053–1073. https://doi.org/10.1080/01431160701281072

Fischer, M. A., Di Bella, C. M., & Jobbágy, E. G. (2015). Influence of fuel conditions on the occurrence, propagation and duration of wildland fires: A regional approach. *Journal of Arid Environments*, *120*, 63–71. https://doi.org/10.1016/j.jaridenv.2015.04.007

Foody, G. (2010). *Assessing the Accuracy of Remotely Sensed Data: Principles and Practices*. *The Photogrammetric Record* (Vol. 25). https://doi.org/10.1111/j.1477-9730.2010.00574_2.x

Gitas, I., Mitri, G., Veraverbeke, S., & Polychronaki, A. (2012). Advances in Remote Sensing of Post-Fire Vegetation Recovery Monitoring - A Review. *Remote Sensing of Biomass - Principles and Applications*. https://doi.org/10.5772/20571

Hoekman, D. H., Vissers, M. A., & Wielaard, N. (2010). PALSAR Wide-Area Mapping of Borneo: Methodology and Map Validation. *IEEE Journal of Selected Topics in Applied Earth Observations and Remote Sensing*, *3*(4), 605–617. https://doi.org/10.1109/JSTARS.2010.2070059

Huang, S., & Siegert, F. (2004). ENVISAT multisensor data for fire monitoring and impact assessment. *International Journal of Remote Sensing*, *25*(20), 4411–4416. https://doi.org/10.1080/01431160412331269670

Kasischke. (1997). The Use of Imaging Radars for Applications A Review Ecological, *4257*(96), 141–156. https://doi.org/10.1016/S0034-4257(96)00148-4

Kasischke, Eric S, Bourgeau-chavez, L. L., French, N. H. F., & Harrell, P. A. (2000). Monitoring Boreal Forests by Using Imaging Radars. In *Climate change and carbon cycling in the boreal forest* (pp. 331–332).

Kavzoglu, T., & Colkesen, I. (2009). A kernel functions analysis for support vector machines for land cover classification. *International Journal of Applied Earth Observation and Geoinformation*, *11*(5), 352–359. https://doi.org/10.1016/j.jag.2009.06.002

Koutsias, N., Karteris, M., & Chuvieco, E. (2000). The use of Intensity-Hue-Saturation transformation of Landsat-5 Thematic Mapper Data for burnt land mapping. *Photogrammetric Engineering and Remote Sensing*, *66*(7), 829–839.

Kumar, S., Khati, U. G., Chandola, S., Agrawal, S., & Kushwaha, S. P. S. (2017). Polarimetric SAR Interferometry based modeling for tree height and aboveground biomass retrieval in a tropical deciduous forest. *Advances in Space Research*, *60*(3), 571–586. https://doi.org/10.1016/j.asr.2017.04.018

Madoffe, S. S., Bakke, A., & Tarimo, J. A. (2000). The effect of fire on the diversity and abundance of wood-living beetles in a miombo woodland, Tanzania. *The Southern African Forestry Journal*, *187*(1), 51–57. https://doi.org/10.1080/10295925.2000.9631256

Menges, C. H., Bartolo, R. E., Bell, D., & Hill, G. J. E. (2004). The effect of savanna fires on SAR backscatter in northern Australia. *International Journal of Remote Sensing*, *25*(22),4857–4871. https://doi.org/10.1080/01431160410001712945

Mouillot, F., Schultz, M. G., Yue, C., Cadule, P., Tansey, K., Ciais, P., & Chuvieco, E. (2014). Ten years of global burnt area products from spaceborne remote sensing-A review: Analysis of user needs and recommendations for future developments. *International Journal of Applied Earth Observation and Geoinformation*, *26*(1), 64–79. https://doi.org/10.1016/j.jag.2013.05.014

Quintano, C., Fernández-Manso, A., & Fernández-Manso, O. (2018). Combination of Landsat and Sentinel-2 MSI data for initial assessing of burn severity. *International Journal of Applied Earth Observation and Geoinformation*, *64*(July 2017), 221–225. https://doi.org/10.1016/j.jag.2017.09.014

Richards, J. A., & Jia, X. (2006). *Remote Sensing Digital Image Analysis*. *Methods* (fifth). Australia: Springer Heidelberg New York Dordrecht London. https://doi.org/10.1007/3-540-29711-1

Roy, D. P., Lewis, P. E., & Justice, C. O. (2002). Burnt area mapping using multi-temporal moderate spatial resolution. *Remote Sensing Letters*, *83*, 263–286.

Sannier, C. A. D., Taylor, J. C., & Du Plessis, W. (2002). Real-time monitoring of vegetation biomass with noaaavhrr in etosha national park, namibia, for fire risk assessment. *International Journal of Remote Sensing*, *23*(1), 71–89. https://doi.org/10.1080/01431160010006863

Siegert, F., & Ruecker, G. (2000). Use of multitemporal ERS2 SAR images for identification of burnt scars in southeast Asian tropical rainforest. *International Journal of Remote Sensing*, *21*(4), 831–837. https://doi.org/10.1080/014311600210632

Sivasankar, T., Srivastava, H., Sharma, P., Kumar, D., & Patel, P. (2015). Study of Hybrid Polarimetric Parameters generated from RISAT-1 SAR data for various Land Cover targets. *International Journal of Advancement in Remote Sensing, GIS and Geography*, *3*(1), 32–42.

Small, D. (2011). Flattening gamma: Radiometric terrain correction for SAR imagery. *IEEE Transactions on Geoscience and Remote Sensing*, 49(8), 3081-3039.

Sun, G., & Ranson, K. J. (2015). Ceos-sar01-074 terrain effect on forest radar backscatter: modeling and correction, (301).

Sunderman, S. O., & Weisberg, P. J. (2011). Remote sensing approaches for reconstructing fire perimeters and burn severity mosaics in desert spring ecosystems. *Remote Sensing of Environment*, *115*(9), 2384–2389. https://doi.org/10.1016/j.rse.2011.05.001

Tanase, M. A., Santoro, M., Aponte, C., & De La Riva, J. (2014). Polarimetric properties of burnt forest areas at C- and L-band. *IEEE Journal of Selected Topics in Applied Earth Observations and Remote Sensing*, *7*(1), 267–276. https://doi.org/10.1109/JSTARS.2013.2261053

Vapnik, V. (2006). Estimation of Dependencies Based on Empirical Data. (M. J. K. Schölkop, Ed.) (Second). Springer NewYork.

Veci, L. (2016). ALOS PALSAR orthorectification tutorial.

Westerling, A. L., Hidalgo, H. G., Cayan, D. R., & Swetnam, T. W. (2006). Warming and Earlier Spring Increase Western U.S. Forest Wildfire Activity, *1161*(August), 940–944.

Yebra, M., Dennison, P. E., Chuvieco, E., Riaño, D., Zylstra, P., Hunt, E. R., … Jurdao, S. (2013). A global review of remote sensing of live fuel moisture content for fire danger assessment: Moving towards operational products. *Remote Sensing of Environment*, *136*, 455–468. https://doi.org/10.1016/j.rse.2013.05.029

Zhu, G., & Blumberg, D. G. (2002). Classification using ASTER data and SVM algorithms; *Remote Sensing of Environment*, *80*(2), 233–240. https://doi.org/10.1016/s0034-4257(01)00305-4